

# The effects of probabilistic context inference on motor adaptation

Cuevas Rivera, Darío<sup>1,2</sup> and Kiebel, Stefan J.<sup>1,2</sup>

<sup>1</sup>Chair of Neuroimaging, Faculty of Psychology, Technische Universität Dresden, 01062 Dresden, Germany.  
<sup>2</sup>Centre for Tactile Internet with Human-in-the-Loop (CeTI)

8 Humans have been shown to adapt their movements when a sudden or gradual change  
9 to the dynamics of the environment are introduced, a phenomenon called motor adapta-  
10 tion. If the change is reverted, the adaptation is also quickly reverted. Humans are also  
11 able to adapt to multiple changes in dynamics presented separately, and to be able to  
12 switch between adapted movements on the fly. Such switching relies on contextual infor-  
13 mation which is often noisy or misleading, affecting the switch between known adaptations.  
14 Recently, computational models for motor adaptation and context inference have been in-  
15 troduced, which contain components for context inference and Bayesian motor adaptation.  
16 These models were used to show the effects of context inference on learning rates across  
17 different experiments. We expanded on these works by using a simplified version of the  
18 recently-introduced COIN model to show that the effects of context inference on motor  
19 adaptation and control go even further than previously shown. Here, we used this model  
20 to simulate classical motor adaptation experiments from previous works and showed that  
21 context inference, and how it is affected by the presence and reliability of feedback, effect a  
22 host of behavioral phenomena that had so far required multiple hypothesized mechanisms,  
23 lacking a unified explanation. Concretely, we show that the reliability of direct contextual  
24 information, as well as noisy sensory feedback, typical of many experiments, effect measur-  
25 able changes in switching-task behavior, as well as in action selection, that stem directly  
26 from probabilistic context inference.

## Introduction

It has been shown that humans can adapt motor commands to counteract changes in the dynamics of the environment and their own bodies, such as performing reaching movements with a weight attached to the wrist. This is known as motor adaptation. Moreover, human participants have been shown to adapt to different, even opposing, changes during the course of a single experiment (Gandolfo, Mussa-Ivaldi, & Bizzi, 1996; Shadmehr & Brashers-Krug, 1997). Additionally, humans have been shown to dynamically switch between different

34 learned adaptations (Davidson & Wolpert, 2004; Ethier, Zee, & Shadmehr, 2008; Lee &  
35 Schweighofer, 2009).

36 By introducing blocks of trials in which body dynamics are altered (e.g. a mechanical  
37 arm exerts a force on the participant's hand), experimenters are able to observe motor  
38 adaptation through the lens of motor error. Across many different motor adaptation exper-  
39 iments (e.g. Davidson & Wolpert, 2004; Gandolfo et al., 1996; Shadmehr & Mussa-Ivaldi,  
40 1994), well-established phenomena have been observed: (i) the ability to recall previously-  
41 learned skills, called savings; (ii) the ability to return to unmodified dynamics, termed  
42 de-adaptation; (iii) the interference in motor learning between opposing manipulations in  
43 dynamics, called anterograde interference; (iv) spontaneous display of behavior consistent  
44 with a previously-learned adaptation, during trials where errors are forced to be zero, called  
45 spontaneous recovery.

46 To explain these phenomena, a number of computational models have been introduced,  
47 which adapt their motor commands after observing motor errors. The most studied are  
48 linear learners (Forano & Franklin, 2020; Scheidt, Dingwell, & Mussa-Ivaldi, 2001; Smith,  
49 Ghazizadeh, & Shadmehr, 2006), but Bayesian accounts have also been presented, providing  
50 an alternative explanation for savings and quick de-adaptation in the form of switching  
51 between forward models (Kording & Wolpert, 2004; Oh & Schweighofer, 2019).

52 While these general models of adaptation explain the most common phenomena observed  
53 in experiments, other known phenomena remain outside of their scope. For example, it is  
54 known that adaptation rate is reduced in situations where the environment is unstable and  
55 unpredictable (Herzfeld, Vaswani, Marko, & Shadmehr, 2014), or situations in which errors  
56 are small (Marko, Haith, Harran, & Shadmehr, 2012) or adaptations slowly introduced  
57 (Huang & Shadmehr, 2009). Action selection has also been found to depend on the history  
58 of adaptations learned (Davidson & Wolpert, 2004; Vaswani & Shadmehr, 2013).

59 Recently, a new computational model for context-dependant motor learning based on  
60 Bayesian inference was introduced by Heald, Lengyel, and Wolpert (2021), called COIN  
61 (for context inference). Heald et al. (2021) formalized context inference as a process that  
62 operates independently from motor learning, but is informed by it, establishing a loop  
63 whereby context inference also informs motor learning. With this model, Heald et al. (2021)  
64 showed that context inference causes the observed changes in the rate of motor learning in  
65 previous experiments (e.g. Herzfeld, Kojima, Soetedjo, & Shadmehr, 2018).

66 In this work show that the process of context inference underlies more behavioral phe-  
67 nomena than previously shown. To do this, we used a minimal model for motor adaptation  
68 that includes context inference, which we derived by simplifying the COIN model (hence-  
69 forth called sCOIN). We focused on the effects of uncertain contextual information on  
70 switching behavior, especially during so-called error-clamp trials, in which errors are forced  
71 to zero by experimenters. More specifically, we focused on the effects of perceptual noise,  
72 as well as feedback modalities, in context inference, which in turn affects behavior in ways  
73 that can be directly measured. We show that through context inference, switching behavior  
74 can display three main effects that have been previously attributed to hypothesized ad-

75 hoc mechanisms: (1) The size of an adaptation dictates how quick and reliable switching  
76 between tasks is (Kim, Ogawa, Lv, Schweighofer, & Imamizu, 2015; Oh & Schweighofer,  
77 2019), which we explain in terms of the effects of perceptual noise on context inference. (2)  
78 Previously-learned adaptations can interfere with switching behavior (Davidson & Wolpert,  
79 2004), which we explain in terms of uncertain context inference. (3) Training history (i.e.  
80 which adaptations have been learned and for how long) affects switching during error-clamp  
81 trials (Vaswani & Shadmehr, 2013), which we also attribute to uncertain context inference.  
82 To do this, we used the sCOIN model to simulate the experimental setups and the decision-  
83 making agents (i.e. participants) during those experiments.

84 Importantly, the goal of this work is not to introduce a new model for contextual motor  
85 learning, but to use the existing ideas of the COIN model to show that context inference  
86 can explain more experimental phenomena than those explored by Heald et al. (2021).

87 With these combined simulations and the qualitative comparison to the experimental  
88 phenomena outlined above, we provide further evidence that context inference is a sin-  
89 gle, coherent and mechanistic account that underlies experimentally well-established motor  
90 adaption and history effects under changing contexts.

## 91 Results

92 Using the sCOIN model, we simulated representative experiments from a number of  
93 experimental studies on motor adaptation to illustrate how this model explains different  
94 experimental findings using the dynamics of context inference. We will present these sim-  
95 ulations alongside the experimental results from the representative studies and discuss in  
96 detail how context inference explains the experimental phenomena.

97 Before presenting these results, we briefly describe the COIN model and the simplifi-  
98 cations that led to the sCOIN version used in simulations. We leave a more thorough  
99 explanation of the models for the methods section. Additionally, we present simulations  
100 using the sCOIN model that show the effects of contextual cues and perceptual noise on  
101 context inference, which pave the way for the simulated experiments that we show later on.

### 102 Modeling context-dependent adaptation

103 We focused on three main components of the COIN model: (1) context inference, (2)  
104 motor adaptation and (3) action selection. The processes defined by these component occur  
105 in this order, and each component informs the ones that follow.

106 Central to the model is the concept of context, defined in terms of the task to be per-  
107 formed, the variables of the environment that are relevant to perform the task, the forward  
108 models used by the decision-making agent to perform the task, and the update mechanisms  
109 necessary to adapt these forward models to the changing environment. Together, these  
110 elements allow the agent to make predictions on future observations when this context is

active, and these predictions are used to infer the context. For example, when lifting an object of unknown weight, an agent might have learned one context for heavy objects and one for light objects. When observing an object to be lifted, the agent can use its size and texture to estimate the weight of the object, which in turn allows the agent to infer the appropriate context and, with it, decide how to lift the object.

The COIN model contains, additionally to these three main components, components for learning new contexts (i.e. inferring the existence of a new context that had not been previously encountered by the agent), as well as the ability to infer subject-specific parameters such as a participant's assumed transition probabilities between contexts, which can differ from the real, hidden transition probabilities. Because we sought to focus on switching behavior between previously-learned contexts, as well as in the perceptual aspect of context inference, we chose to fix the participant-inferred transition probabilities between contexts, as well as the total number of contexts; in our simulations, we assume that participants have already inferred the real values of these quantities. Because we mainly focus on switching behavior, as well as error-clamp trials (both of which involve already-learned adaptations), these simplifications to the model have minimal effects on our results. See Methods for more details on the sCOIN model, as well as the differences between COIN and sCOIN.

By fixing the aforementioned values, the sCOIN model has a simpler generative model which allows the agent to perform exact Bayesian inference for motor adaptation. The inference process can be seen in Figure 1A, including the priors for both context inference and motor adaptation. For more details on these choices, see the Methods section.

### Contextual cues and feedback

The behavioral phenomena which are the focus of this work can be explained as arising from the effects of contextual cues and sensory feedback provided to participants during the experiment. To illustrate these effects in a simple example, we first simulated a generic motor adaptation experiment similar to those performed by Davidson and Wolpert (2004), in which participants must adapt to the curl forces exerted by a mechanical arm on the participants' hands as they perform pointing movements.

The key to an intuitive understanding of the results presented below is to observe what happens when the presence and reliability of contextual cues is varied, as well as the perceptual noise on the position of the hand. In Figure 1B, a 2x2 grid of results is shown: each simulation in this grid is a combination of low or high contextual cue uncertainty (where high uncertainty is equivalent to presenting no cues), and low or high perceptual noise (representing how well participants can detect deviations from the straight-line movements).

Figure 1B shows that, in the presence of reliable contextual cues, context inference is accurate, certain and fast to switch. However, as contextual cues become less reliable, switching between known contexts becomes slower, as seen in the posterior probabilities over contexts at and after trial 20 in the last column. Furthermore, as perceptual noise increases, switching becomes not only slower, but also more uncertain, with individual

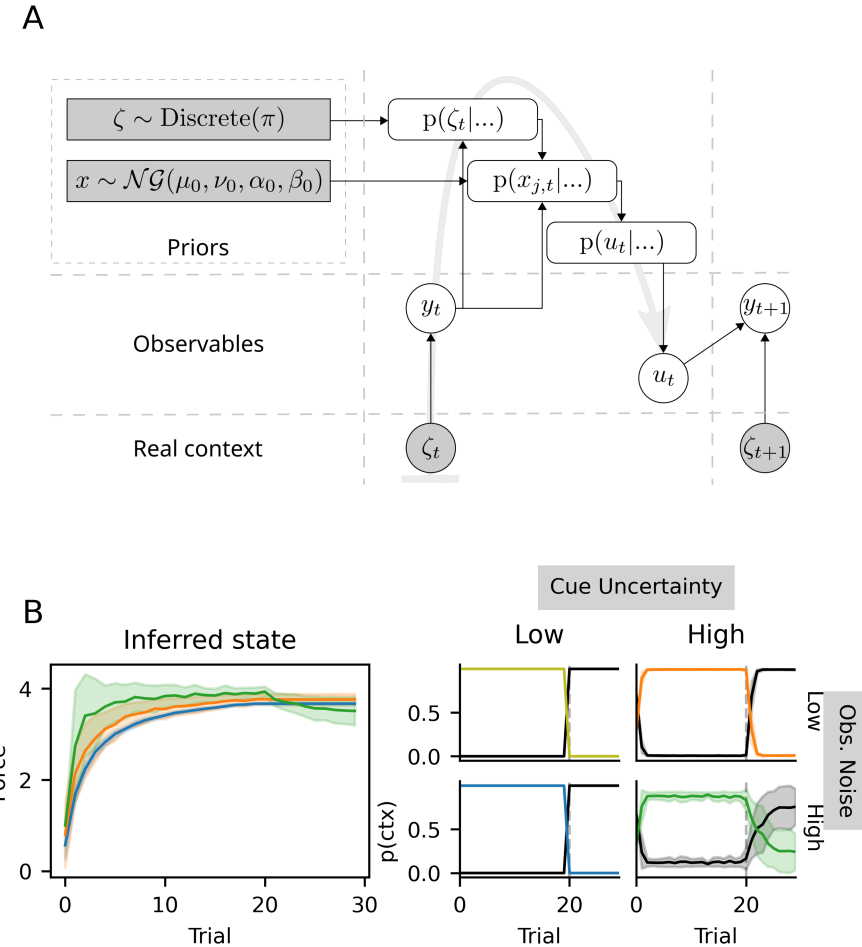


*Figure 1.* Schematic representation of the model and illustrative simulations. (A) Inference done by the model at every trial. Clear circles represent the observables, i.e. motor commands  $u_t$  and direct observations  $y_t$  (e.g. cursor position). The true context  $\zeta_t$  is not directly observable, but influences  $y_t$ . The dark rectangles represent the prior distributions for the inferred adaptation level  $x_t$  (Normal-Gamma distribution) and the current context  $\zeta_t$  (discrete distribution with known  $\pi$ ; see Methods). At every trial, the context is inferred, then motor adaptation is carried out and finally a motor command is issued; the flow of this process is indicated by the gray arrow in the background, while black arrows show the direction of information flow. (B) Simulations obtained with the model in (A), using a simulated experimental setup similar to that by Davidson and Wolpert (2004), in which the context changes at trial 20 (vertical, dashed lines). A total of 2x2 experiments were simulated, with low and high levels of both cue uncertainty and observation noise. In the left panel, the states inferred by the model for each of the 2x2 simulated experiments, where each color represents one experiment, with the same colors as the panels on the right. On the right, each plot represents context inference  $p(\zeta_t)$  for one specific level of cue uncertainty and observation noise. The y-axis represents the posterior probability of each context  $p(\zeta_t = j)$ ; the black line represents the baseline context (i.e. no adaptation), the colored line (with the same colors as the panel on the left) represents the only adaptation to be learned during the simulated experiment. The shaded areas represent the standard deviation around the mean, obtained across 50 simulated participants.

agents incorrectly missing the switch entirely. While cue uncertainty and observation noise have an effect on the motor adaptation process, as seen on the left-most panel in Figure 1B, in all simulations the hidden state (i.e. the force exerted by the mechanical arm,  $x_{j,t}$ ) is quickly inferred.

As we show below, these effects are at the heart of the behavioral phenomena observed in the experiments by Kim et al. (2015), Oh and Schweighofer (2019), Davidson and Wolpert (2004), and Vaswani and Shadmehr (2013), which we directly simulate in this work, alongside others that we discuss in the Discussion section.

## Experimental results

In this section, we present experimentally-observed phenomena in three sections, and show that the dynamics of context inference provide a unifying explanation for all of them. In the first section, we discuss switches between contexts, and how slow context inference affects these switches. In the second section, we focus on interference between learned adaptations. Finally, in the third section we discuss context inference during error-clamp trials, and its effect on behavior. For each of the three sections, we selected one or two studies which are representative of the phenomenon being discussed.

For clarity, we first introduce necessary terminology that is typically used in experimental studies. As an example, we will use a typical motor adaptation task in which participants have to make reaching movements while holding the handle of a mechanical arm that exerts a curl force on the participant's hand. Depending on the trial, the mechanical arm might exert a curl force in a clockwise or counter-clockwise direction, or no force at all. Let us define the baseline context  $O$  as that in which the mechanical arm exerts no force. Contexts  $A$  and  $B$  can be defined as those with clockwise and counter-clockwise forces, respectively. Abusing notation, a usual statement is that  $B = (-A)$ , as the forces have the same magnitude but point in opposite directions. Similarly, one can define context  $A/2$ , with the same direction of adaptation as  $A$ , but half the magnitude. Finally, many experiments include a block of error-clamp trials at the end of the experiment, in which the mechanical arm forces the participant to make straight-line movements; we represent these with the letter  $E$ .

With this terminology, a typical experiment (e.g. Ethier et al., 2008) would have a block structure of  $O - A - B - E$ , or  $O - A - (-A) - E$ , which means that the participant goes through a block of trials with no external force applied ( $O$ ), a number of trials with a clockwise curl force ( $A$ ), a block with counter-clockwise forces ( $B$ ), and finally a block with error-clamp trials ( $E$ ). With repeated contexts (e.g. Oh & Schweighofer, 2019), an experiment can be described as  $O_1 - A_1 - O_2 - \dots$

**Cue- and sensory feedback uncertainty affects switching behavior.** The term 'savings' refer to the ability to remember a previously-learned adaptation and apply it without having to re-learn it. Savings is almost universally observed in humans (Brashers-Krug, Shadmehr, & Bizzi, 1996; Medina, Garcia, & Mauk, 2001; Shadmehr & Brashers-Krug, 1997; Smith et al., 2006; Zarahn, Weston, Liang, Mazzoni, & Krakauer, 2008). In an

189  $O - A - O - A$  experiment, for example, savings would express themselves in the second  
190 A block in the form of a much higher adaptation rate than that observed during the first  
191 A block. The related concept of quick de-adaptation occurs in  $A - O$  transitions, where  
192 participants switch back to baseline without having to re-learn it.

193 In this section, we discuss savings in terms of switching between contexts. We show that  
194 through context inference and how it is affected by contextual cues and observation noise,  
195 savings are not immediate, but a relatively fast process that reflects context inference. In  
196 particular, we show that the manifestations of savings on behavior are mediated by context  
197 inference, which could mask the presence of savings in cases where observations do not  
198 unequivocally identify a context.

199 To show this, we examined multiple experimental studies in which savings are observed.  
200 We categorized these studies based on the amount of contextual information made available  
201 to participants: In some experiments (e.g. Kim et al., 2015; Lee & Schweighofer, 2009), the  
202 context is clearly revealed to the participant using sensory cues. We call these cued-context  
203 experiments. In other experiments, partial information is available to participants (e.g.  
204 Davidson & Wolpert, 2004; Zarahn et al., 2008) in the form of large prediction errors,  
205 partial contextual information or reward prediction errors; we refer to these as partially-  
206 cued experiments.

207 We selected three representative experiments from two studies (Kim et al., 2015; Oh &  
208 Schweighofer, 2019) which differ in the amount of contextual information available to par-  
209 ticipants. Kim et al. (2015) performed a cued-context visuomotor rotation experiment with  
210 three contexts with different rotation: no rotation, 40 degrees and -40 degrees. Participants  
211 performed shooting movements in blocks of trials with the same rotation. Importantly, a  
212 colored light identified the current context, making this a cued-context experiment. Con-  
213 sistent with the context-inference account, the authors found that switching was immediate  
214 and accurate.

215 In Figure 2A we show the results of simulations with the model using the parameters  
216 of the task, as well as the experimental results from Kim et al. (2015). The correspon-  
217 dence between simulations and experimental results can be seen in the switches between contexts  
218 in the center panel, i.e. when the solid gray line (representing the true context) switches  
219 between 40, 0 and -40; in the two right-most panels, the thick black line, representing the  
220 agent’s adaptation, quickly follows these switches.

221 In the second panel of Figure 2A, we show the inferred state (i.e. the inferred angle  
222 of rotation). Critically, it can be seen for the first four context switches (until about trial  
223 200) that participants had not yet completely adapted to the rotation, as also evidenced  
224 by their responses not being on par with the true rotation angle. This undershooting of  
225 responses (i.e. not doing the 40 degree rotation) happens despite participants being able to  
226 immediately and with high certainty identify the true context, as shown in the first-column  
227 panel. These results are similar to those shown by Imamizu et al. (2007), where sensory  
228 cues of varying reliability effected immediate or slow contextual switches.

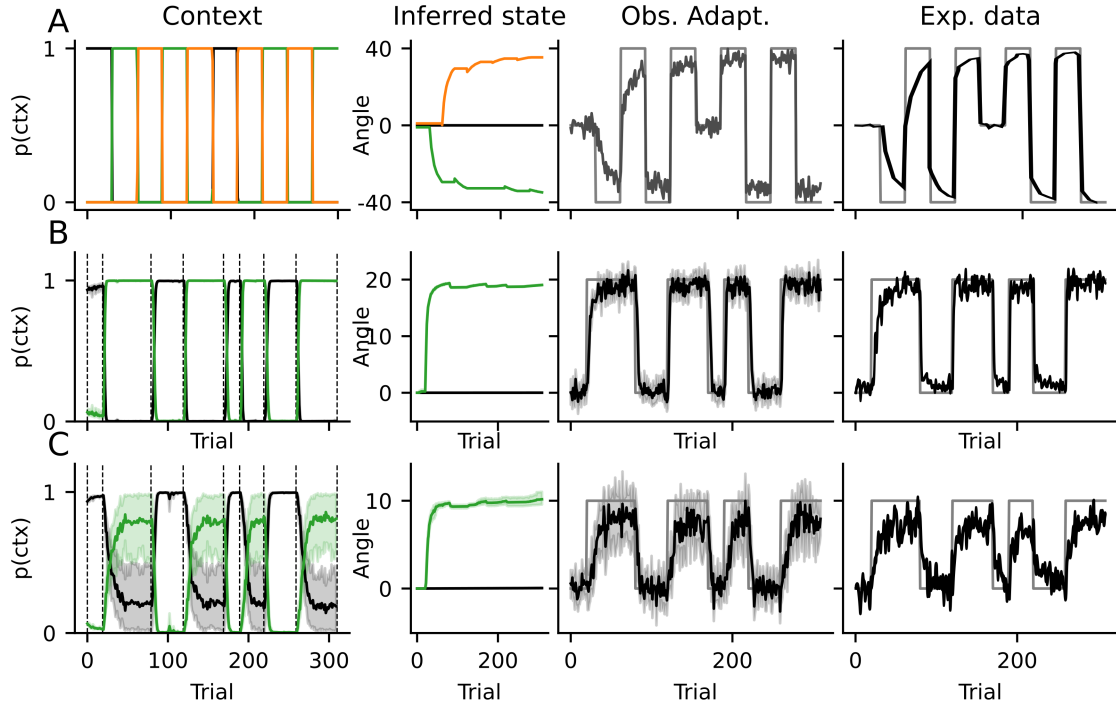


*Figure 2.* Switching between learned adaptations gated by context inference. Data from our simulations (first three columns) compared to data adapted from figure 2A by Kim et al. (2015) and figure 4A from Oh and Schweighofer (2019) (last column). Experimental and simulated data was, in all three experiments, averaged across all participants. In the first column, the simulated context inference is represented by the posterior probabilities over all available contexts. Each color (black, blue, green) represents a different context, with black always representing the baseline (i.e. no adaptation). Vertical, dashed lines represent switches in the real context. The inferred state (angle of the visuomotor rotation) is shown in the second column, with the same colors as in the first column. In the third and fourth columns, the black line represents the adaptation (i.e. response) displayed by the agent as a function of trial number. The thin gray lines represent the optimal adaptation, i.e. the size of the true visuomotor rotation during the task. (A) Experiment by Kim et al. (2015). Both experimental and simulated results are shown only up to trial 300, of the original 600. (B) An experiment by Oh and Schweighofer (2019). Blue and black lines are as in A. (C) Same experiment as (B) but with a 10 degree adaptation.

To expand on these results, we now turn to feedback and its effects on switching behavior. Oh and Schweighofer (2019) performed two partially-cued experiments with a visuomotor rotation of 20 and 10 degrees, respectively. The results of their experiments can be seen in Figure 2B and 2C, alongside simulations with the sCOIN model. Participants in the first experiment (Figure 2B) first learned the adaptation in  $A$ . In subsequent context transitions, participants showed immediate switching (with a one-trial lag) between  $A$  and  $O$  (both ways), which can be seen in their responses (black line in the last two columns of Figure 2B) closely following the switches in the true rotation. In the second experiment (Figure 2C), context switching happens more slowly, with adaptation lagging behind the switches in the real context, and slowly catching up. As can be seen in the left panels in Figure 2B and 2C, the same model parametrization produces fast, accurate switches when the adaptation is large (B), and slow, noisy switches when it is low (C). This difference is explained in our simulations in terms of the size of the adaptation in relation to observation noise: as the adaptation is smaller (10 degrees), it becomes more difficult to distinguish errors made by incorrectly inferring the context from the noise due to trial-to-trial variation in motor output. Because of this, the model requires more evidence (i.e. more trials) to infer a switch in contexts.

In contrast, Oh and Schweighofer (2019) explained the results of their second experiment by positing that when adaptations were small, participants did not identify this as a new context and opted instead for a modification of their baseline model (i.e. how they move normally). Under this single-context explanation, however, savings do not exist, and adaptations need to be learned anew every time a context changes. On the other hand, savings are present under the sCOIN model, their manifestations being diminished by the slower context inference. Oh and Schweighofer (2019) analyzed savings during their second experiment and found that savings do exist, although greatly diminished compared to the first experiment. This is in favor of the dual-context model, as we present it here. Oh and Schweighofer (2019) showed a slow decay during error-clamp trials in their experiments, which they considered evidence for the single-context account of the second experiment. However, as we show below, this can also be explained in a dual-context model as an effect of slow context inference.

**Uncertainty over contexts affects action selection.** As with learning, we show in this section that action selection is affected by context inference. If the identity of the current context is known, the forward model for this context is used to select the current action. However, if uncertainty over the context exists, the selected action is influenced by all the possible contexts, with a weight directly related to how likely each one of those contexts is (see Equation 6).

Experimental evidence supporting this view can be found in experiments with context switching. For example, Davidson and Wolpert (2004) reported a curl-force experiment in which participants had to switch between  $A$  and  $3A$  in one group, with a block sequence  $A - 3A - A - 3A$ , and from  $A$  to  $-A$  in another group, with a block sequence  $A - (-A) - A - (-A)$ . After  $A$  and  $3A$  (or  $-A$  in the other group) had been learned in the first two blocks, the authors found that the switch from  $3A$  to  $A$  was faster than that from  $-A$  to  $A$ . The authors interpreted this as evidence that switching between adaptations happens more

272 quickly if it is in the same direction as the current adaptation (e.g. both counter-clockwise),  
 273 and more slowly if they are in the opposite direction (e.g. clockwise to counter-clockwise).

274 Under the sCOIN model, the asymmetry is caused by the existence of the baseline  
 275 context, which has a non-zero probability  $p(\zeta_O|s_t\dots)$ , as can be seen in Figure 3A. When a  
 276 new block of trials starts (e.g. in the transition from 3A to A), a switch is inferred by the  
 277 model (given feedback after the first trial) and  $\zeta_O$  becomes more likely (given that  $\zeta_{3A}$  has  
 278 been ruled out). Therefore, in these first trials, action selection has a component guided by  
 279 the baseline model, in which no extra compensatory force is applied, effectively “pulling”  
 280 adaptation towards zero (no compensatory force). In the first group, this initial pull towards  
 281 zero accelerates the transition towards A because  $3A > A > 0$ , but in the second group,  
 282 it slows down the switch because  $A > 0 > -A$  and the behavior lingers around 0 until  
 283  $p(\zeta_0|\dots)$  drops back to zero.

284 To confirm this explanation, we simulated variants of the experiment in which the sCOIN  
 285 model predicts that the difference between groups diminishes or disappears. First, in Fig-  
 286 ure 3B, we simulated an experiment in which the contexts have more extreme adaptations,  
 287 making them more different from baseline than in the Davidson and Wolpert (2004) ex-  
 288 periments. To do this, one group adapts in a  $O - A - (-2A)$  paradigm, while the other  
 289 group adapts in a  $0 - A - 4A$  paradigm. As in the original experiment, the second contexts  
 290 ( $-2A$  for one group,  $4A$  for the other) are equally spaced from the first context. However,  
 291 given the larger distance from baseline, the baseline context has the same probability for  
 292 both groups after the switch back to A. This change makes both simulated groups infer  
 293 the correct context almost equally quickly, making the difference between their errors much  
 294 smaller compared to the original experiment. Furthermore, we simulated an experiment  
 295 with an identical structure to that of Davidson and Wolpert (2004), but eliminated the  
 296 baseline context from the agent. The results can be seen in Figure 3C, where the switches  
 297 between contexts are made identically by the two groups.

298 **Action selection in error-clamp blocks.** During error-clamp blocks at the end  
 299 of block sequences, participants’ behavior can be divided in two phases: (1) Participants’  
 300 behavior is consistent with a previously-encountered context (called spontaneous recover  
 301 in  $O - A - B - E$  experiments, where behavior is consistent with A); this phase, when  
 302 present, is seen during the early trials of the E block. (2) A slow return to baseline, which  
 303 can last as long as hundreds of trials (Brennan & Smith, 2015). However, the direction of  
 304 adaptation during the first phase, its duration, the delay before it is observed, the speed of  
 305 the return to baseline and the final asymptote of the response vary greatly depending on  
 306 the experiment (Brennan & Smith, 2015; Shmuelof et al., 2012; Smith et al., 2006; Vaswani  
 307 & Shadmehr, 2013).

308 In this section, we show how context inference can explain these different parameters  
 309 of behavior by changing the way contextual cues mislead participants’ context inference,  
 310 which in turn influences action selection.

311 This can be seen for example in (Vaswani & Shadmehr, 2013), where the authors studied  
 312 in detail human behavior during an error-clamp block in a shooting movement paradigm

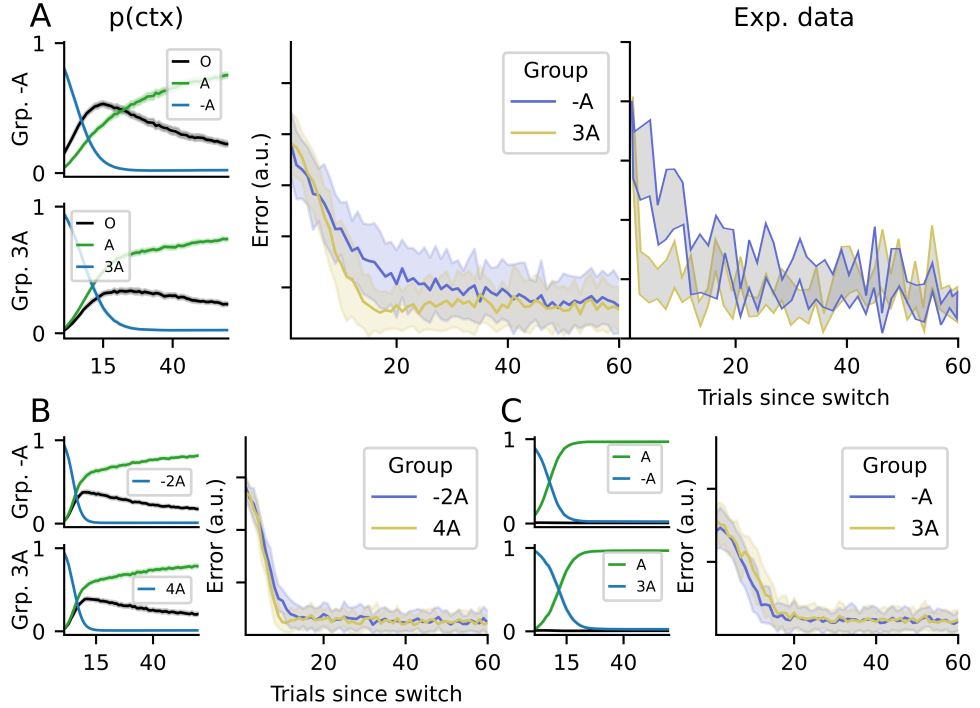


*Figure 3.* Motor error when switching back to a previously-learned adaptation. (A) Experimental results from Davidson and Wolpert (2004) and simulations with the SCION model are shown. In the first column, each panel represents context inference for one group of participants (top: group A; bottom: group 3A), with each line representing the posterior probability of a context (black for the baseline O). The second column represents the error made by our simulated agent after returning to the previously-learned context, with blue and yellow representing groups -A and 3A, respectively. The last panel represents the same data, from the Davidson and Wolpert (2004) experiment. All panels share the x-axis, representing the number of trials elapsed since the switch to the new context. All simulations were executed 32 times per group, to obtain a reliable mean; shaded areas represent the standard deviation across all simulations. (B) Simulated results for an experiment similar to Davidson and Wolpert (2004), but changing the contexts seen by the two groups from -A to -2A for the first group, and from 3A to 4A for the second group. The panels follow the same structure as (A), without the last panel for experimental results. (C) Simulations for an experiment in which the baseline context has been removed altogether.

with a mechanical arm. The authors found that during an  $E$  block at the end of each experiment, there was a lag of a few trials (depending on participant) before their motor behavior changed from that of the previous block. After that, the exerted force slowly dropped towards zero throughout tens of trials, but never reaching values around zero. Participants were divided into four groups, each of which going through a different block sequence: (1.1)  $A - E$ , (1.2)  $O - A - E$ , (1.3)  $(-A/2) - A - E$ , and (1.4)  $(-A) - E$ . No pauses were made during the experiment nor were there any contextual cues, so transitions between blocks were not signaled to participants. However, because context inference integrates information from different sources, many experiments in which no intentional, overt contextual cues are available indeed contain contextual information that the participant can use to infer the context. For example, proprioceptive signals provide contextual information (Dizio & Lackner, 1995; Shadmehr & Mussa-Ivaldi, 1994). The sudden appearance of motor errors can itself be a cue for contextual change (Herzfeld et al., 2014) and even a pause between two trials could suggest a change in context (Ethier et al., 2008).

In Figure 4A, we show data simulated with the sCOIN model, following the parameters of the experiment by Vaswani and Shadmehr (2013), and in Figure 4B we show the experimental plots adapted from Vaswani and Shadmehr (2013). As in the experiments by Vaswani and Shadmehr (2013), we simulated error-clamp trials by forcing the observed error to zero, regardless of the action taken by the model. The displayed adaptation is shown during the  $E$  trials for the three experimental groups in the experiment. It can be seen that group 1.3 (i.e. the participants who had learned in the  $-A/2$  context in addition to  $A$ ) more quickly recognized a change in context and lowered the force applied on the mechanical handle, as can be seen in the experimental data.

In Figure 4C, the inference over context is shown for each group separately. Context inference works reliably until the error-clamp trials start, which do not correspond to any of the known contexts. This causes the agent to infer the combination of some of the known contexts that best fits the observations. Depending on the contexts previously learned by the agent: groups 1.1 and 1.4 display the same behavior, where the previous context ( $A$  and  $-A$ , respectively) slowly dwindles. These agents will slowly lower the force applied. In contrast, group 1.3 has learned the additional  $-A/2$  context, which has a non-zero posterior probability during  $E$  trials, pushing the agent's adaptation force more quickly towards zero. Group 1.2 behaves similarly to 1.1, with the exception that the baseline context, which was recently seen, plays a bigger role during  $E$  trials, making the agent reduce its force during  $E$  trials slightly more quickly than groups 1.1 and 1.4.

Vaswani and Shadmehr (2013) also found participant-specific delays before the decay to baseline started after the error-clamp phase begun. As can be seen in Figure 4D, each simulated participant follows a different path of decay, with variations caused directly by perceptual noise. In our simulations, however, it is clear that no such systematic lag can be directly observed, which is most noticeable when looking at context inference (Figure 4C), which begins the switch as soon as the error-clamp trials begin. This can be further observed in Figure 4D, where we plot each simulated participant (one run of the simulations, color coded as before); because observation noise was chosen randomly for each run, some

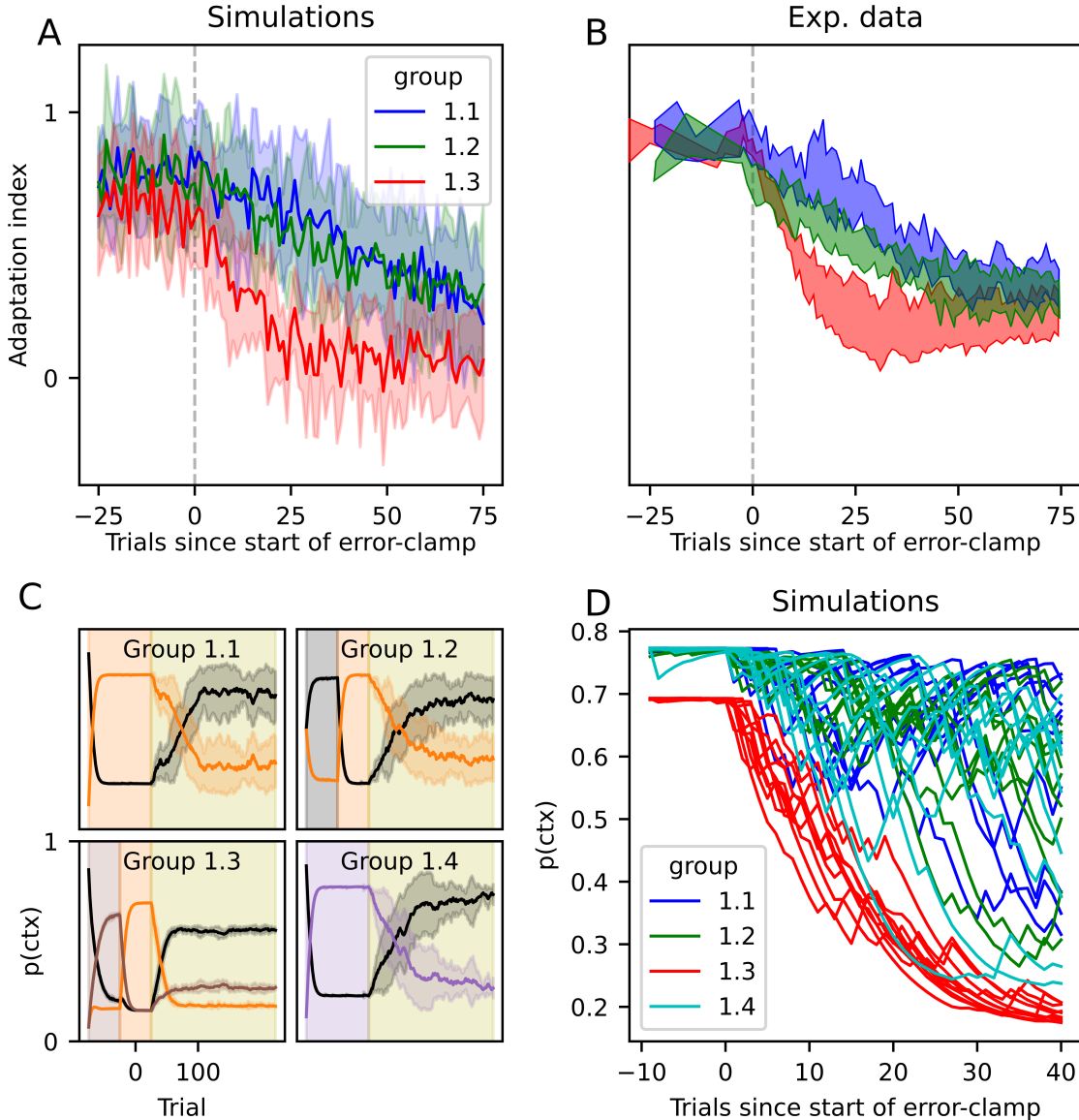


*Figure 4.* Adaptation during error clamp trials. (A) Simulated adaptation during the error-clamp trials for the three groups of participants in Vaswani and Shadmehr (2013), using the same colors. Following Vaswani and Shadmehr (2013), group 1.4 is not shown in A and B, as their behavior is identical to group 1.1. The solid line is the average across 10 runs (i.e. a group of 10 simulated participants) and the shaded area represents the standard deviation. The vertical dashed line is the start of the error-clamp trials. (B) Corresponding experimental data adapted from figure 2C by Vaswani and Shadmehr (2013). (C) Simulations: Inference over the current context, where contexts are color coded: black for baseline, orange for the counter-clockwise force, purple for the clockwise force and brown for counter-clockwise force with half strength. The lines represent the posterior probability of each context in every trial, while the background color represents the true context. An olive-colored background represents error-clamp trials. As in (A), solid lines represent the average across all runs and shaded areas represent the standard deviation. (D) Simulations: Visualization of the lag before a change in context is detected by the agent during the  $E$  trials. Each line represents one run (10 runs per group).

355 runs appear to contain a large delay before the decay begins. This falls in line with the  
356 experiments by Brennan and Smith (2015), who found that the lag observed by Vaswani  
357 and Shadmehr (2013) disappeared when controlling for correlations in perceptual noise, as  
358 well as by using a balanced experimental design and unbiased analysis.

359

## Discussion

360 We showed that context inference as an active, continuous process, can explain many  
361 behavioral phenomena observed experimentally. In particular, we showed that the effects  
362 of the presence and reliability of contextual cues, as well as observation noise, can cause  
363 behavior that can be observed during context switching, as well as during times in which  
364 context inference is hindered, as is the case during error-clamp trials in many experiments.

365 To do this, we selected representative experimental studies that show the well-established  
366 effects of savings, spontaneous recovery and the effects of sensory cues. Using a simplified  
367 version of the COIN model introduced by Heald et al. (2021), we showed how each of  
368 these effects can be explained by the dynamics of context inference, which integrates all the  
369 available information (e.g. sensory cues, workspace location, reward and endpoint feedback),  
370 in some cases throughout many trials.

371 With this, we expanded on previous works that introduced the idea that context in-  
372 ference is a process that informs and is informed by motor adaptation by showing that  
373 it explains behavioral phenomena that had previously required different specific, ad-hoc  
374 mechanisms outside of contextual motor adaptation.

375 **Further experimental evidence**

376 In many cases, the context is not directly observable and context inference takes the  
377 form of an evidence-accumulating process that can take any amount of time to be sure of  
378 the context. It is in these cases where the effects of context inference are most noticeable.  
379 While many experiments exist that give probabilistic contextual information (e.g. Behrens,  
380 Woolrich, Walton, & Rushworth, 2007; Nassar, McGuire, Ritz, & Kable, 2019; Scholz &  
381 Schöner, 1999), evidence accumulation is not limited to these explicitly stochastic cases.  
382 Indeed, as we noted in the Results section, many experiments inadvertently include partial  
383 contextual information used by participants.

384 The most direct secondary contextual information comes in the form of reward and end-  
385 point feedback. For example, participants may be told whether they obtained the desired  
386 reward at the end of a trial and are shown the end point of their movement. When partic-  
387 ipants observe an unexpectedly large error, they can infer that the inferred context might  
388 be incorrect. This is the case of the experiments by Oh and Schweighofer (2019) shown  
389 in Figure 2B-C: if the adaptation is high, changes in context produce errors much larger  
390 than those of motor variability, and a context switch is easily and immediately identified;

391 if adaptation is low, the errors produced by context switching are closer in magnitude to  
392 motor variability and evidence accumulation is necessary.

393 The same rationale explains the results by Herzfeld et al. (2014), as was shown by Heald  
394 et al. (2021): motor learning, which in the COIN model is modulated by context inference,  
395 is minimal for errors close to 2 and -2 (see their figure 2E). This is because an error of  
396 2 or -2 signals that the participant incorrectly identified the context (as adaptation has  
397 a magnitude of 1). Additionally, as was shown by Heald et al. (2021), context inference  
398 explains the modulation of learning rate by the volatility of the environment observed by  
399 Herzfeld et al. (2014).

400 A subtler source of information can be found in long pauses between blocks of adaptation  
401 trials, after which an unprompted partial return to baseline has been observed (Ethier et al.,  
402 2008). This can be explained by context inference, as a long pause could prompt participants  
403 to infer that a switch had occurred, prompting participants to rely on their belief of the  
404 underlying probability of observing any of the known contexts, which is dominated by the  
405 previously observed context *A*, but now includes a component of the baseline *O*, as it is the  
406 most common one in everyday life.

407 Error-clamp (*E*) trials present another insight. If error is kept at zero, one could assume  
408 that participants would continue doing what they were doing before, as there is no reason  
409 (no observed error) to infer a change in context. However, this is almost never the case (e.g.  
410 Ethier et al., 2008; Forano & Franklin, 2020; Pekny, Criscimagna-Hemminger, & Shadmehr,  
411 2011; Scheidt, Reinkensmeyer, Conditt, Rymer, & Mussa-Ivaldi, 2000; Smith et al., 2006;  
412 Vaswani & Shadmehr, 2013). Instead, participants slowly reduce their adaptation, often  
413 displaying spontaneous recovery (e.g. Smith et al., 2006). Context inference provides a prin-  
414 cipled account of this behavior: the natural variability in participants' behavior lead them  
415 to expect errors, which clashes with the observed zero error. This prompts participants to  
416 re-evaluate their inferred context, which can partially activate a previously-observed con-  
417 text, as we showed in Figure 4. Pekny et al. (2011) found similar results, demonstrating  
418 that the duration of the previously-observed adaptation block also affects behavior in the *E*  
419 block. Additionally, Criscimagna-Hemminger and Shadmehr (2008) showed that introduc-  
420 ing long periods before the *E* block begins lowers the initial force that participants exerted  
421 on the mechanical arm during the *E* block; longer periods of time make context inference  
422 revert to the prior expectation that a new baseline block begins, because participants are  
423 free to move their arm about during the pause.

424 In our account, if all information indicating a change in context is removed from the  
425 experiment, participants would continue to behave as they were in the previous block.  
426 Evidence for this can be seen in experiments 2 and 3 by Vaswani and Shadmehr (2013),  
427 where participants were shown random errors during *E* trials, with a variance matching  
428 that of previously observed motor commands. The authors showed that by matching the  
429 errors expected by participants, they eliminated the slow tapering-off observed in most *E*  
430 blocks.

431 **Model predictions**

432 The basic principle behind the results we presented is that the sCOIN model describes  
433 a process that develops over time and that carries with it uncertainty. This uncertainty  
434 affects learning and behavior during motor adaptation, effecting phenomena that are directly  
435 observable during behavioral experiments. In the following, we discuss several testable  
436 predictions that are direct consequences of the model.

437 For the model predictions discussed below, it is important to keep in mind that different  
438 contextual cues are not equally effective at separating motor responses during learning and  
439 switching (Howard, Ingram, Franklin, & Wolpert, 2012; Howard, Ingram, & Wolpert, 2010;  
440 Imamizu et al., 2007). Because of this, the model predictions hinge on selecting the adequate  
441 type of contextual information that maximally helps the participants select the appropriate  
442 motor response.

443 **Error-clamp as a known context.** The inclusion of reliable sensory contextual cues  
444 (e.g. lights whose color uniquely identify a context) makes switching immediate, as in the  
445 experiments by Kim et al. (2015). We expect that the same effect would be observed in  
446 error-clamp trials. If the *E* block is learned by participants during training, it might still  
447 be difficult for them to infer that an *E* block has started, which would create delays similar  
448 to those in Figure 4. However, the model predicts that if a visual cue is introduced that  
449 identifies the *E* block, participants would immediately switch to their baseline behavior, no  
450 longer displaying an adapted response, lag, nor the slow return to baseline. This imme-  
451 diate switch in the presence of contextual cues would persist even if endpoint feedback is  
452 manipulated as Vaswani and Shadmehr (2013) did.

453 Note that the original COIN specification includes a component to learn new contexts.  
454 However, this component works exclusively by creating new contexts in which the forward  
455 models take the same form but have different parameter values. New mechanisms would  
456 be needed to allow the COIN model to create contexts in an online fashion that operate in  
457 an essentially different manner, as is the case of error-clamp trials, in which participants'  
458 responses do not affect the outcome and motor commands are issued based on criteria not  
459 directly related to the goal of the task (e.g. energy minimization or comfort maximization).

460 **Interference effects during context switching.** As discussed in the Results section,  
461 the effect observed by Davidson and Wolpert (2004) is explained by the model as an effect  
462 of slow context inference, instead of being a direct interference at the level of learning.  
463 As shown in Figure 3B-C, the context inference account predicts that this effect would  
464 disappear if all contexts were significantly different from baseline, such that the baseline  
465 context never explains the observations. Removing the baseline context from a participant's  
466 context inference might be experimentally unfeasible, but other possibilities include making  
467 all adaptations bigger (e.g. bigger angles, stronger forces), and including contextual cues  
468 that rule out the baseline context. In the opposite direction, the model predicts that if  
469 all adaptations are smaller (i.e. closer to baseline), the differences between the two groups  
470 would increase, although such differences might become impossible to detect due to different

471 sources of noise in the data.

472 **Multi-source integration.** The model also predicts an effect reminiscent of multi-  
 473 sensory integration (Ernst & Banks, 2002): in order to integrate contextual information  
 474 from conflicting sources (e.g. probabilistic visual cues and noisy endpoint feedback), the  
 475 weight placed on a source increases with its reliability. Such integration would manifest  
 476 itself in experiments in which observations are noisy, as in the experiments by Kording and  
 477 Wolpert (2004), in which the position of the finger was obscured and instead participants  
 478 are shown a blurry cursor which was sometimes shifted from its real position. If the added  
 479 observation noise gives evidence for a particular context (the true underlying context or an-  
 480 other one) and a visual cue gave partial information for another context, the participants'  
 481 behavior would be more consistent with the most reliable source of contextual information.

## 482 Conclusions

483 The results we presented in this work indicate that several well-established behavioral  
 484 phenomena observed across different motor adaptation experiments can be explained by the  
 485 uncertainty in context inference and its effects on learning and action selection. Together  
 486 with the results by Heald et al. (2021), these results suggest new venues of investigation for  
 487 future works in motor adaptation and context-dependent behavior.

## 488 Methods

### 489 The COIN and sCOIN models

490 In this work, we used a simplified version of the recently-introduced COIN model (Heald  
 491 et al., 2021), adapted to the experiments that we covered in our simulations. In this section,  
 492 we give a brief introduction to the COIN model and, in the subsequent subsection, describe  
 493 how we adapted the model to the experimental tasks. For a full description of the model,  
 494 refer to Heald et al. (2021).

495 **Generative model.** At each trial  $t$ , the agent infers both the context and the context-  
 496 dependent adaptation (e.g. the parameters of the force field in mechanical-arm experi-  
 497 ments). The context is represented by a latent, categorical variable  $\zeta_t$ , which is assumed to  
 498 evolve over time according to:

$$p(\zeta_t | \zeta_{t-1}, \pi_{\zeta_{t-1}}) = \text{Discrete}(\pi_{\zeta_{t-1}}) \quad (1)$$

499 where  $\pi_{\zeta_{t-1}}$  is the transition probability vector from context  $\zeta_{t-1}$  to all other contexts. The  
 500 contextual cues (when present in an experiment) are assumed to be drawn depending on  
 501 the context following:

$$p(q_t | c_t, \Phi) = \text{Discrete}(\Phi_{\zeta_t}) \quad (2)$$

502 where  $\Phi_{\zeta_t}$  is the probability vector with which the contextual cue  $q_t$  is shown to the agent  
 503 in context  $\zeta_t$ . As pointed out by Heald et al. (2021), both  $\Phi$  and  $\pi$  are in principle infinite,  
 504 but a task-relevant finite set can be used instead.

505 The context-dependent adaptation is represented by the latent variable  $x_{\zeta,t}$  and assumed  
 506 to arise from an autoregressive process AR(1):

$$x_{\zeta,t} = a_{\zeta}x_{t-1} + b_{\zeta} + \omega_{\zeta} \quad (3)$$

507 where  $a_{\zeta}$  and  $b_{\zeta}$  are unknown, context-dependent parameters and  $\omega$  is a Gaussian noise  
 508 term of zero mean and unknown standard deviation  $\sigma_{\zeta,x}$ . This AR(1) process is assumed to  
 509 have existed before the experiment begins and to have a stationary Gaussian distribution  
 510 of unknown mean and variance:

$$p(x_{\zeta,t}) = \mathcal{N}(\mu_{\zeta,x}, \sigma_{\zeta,x}) \quad (4)$$

511 Note that  $\mu_{\zeta,x}$  and  $\sigma_{\zeta,x}$  are parametrized by the parameters of the AR(1) process, namely  
 512  $\mu_{\zeta,x} = d_{\zeta}/(1 - a_{\zeta})$  and  $\sigma_{\zeta,x} = \sigma_q/(1 - a_{\zeta}^2)$ , where  $\sigma_q$  is a free parameter of the model which  
 513 is not context dependent.

514 Observations take the form of state feedback (e.g. the position of the cursor on the  
 515 screen in visuomotor rotation tasks), given by:

$$y_t = x_{\zeta,t} + \nu_t \quad (5)$$

516 where  $\nu_t$  is a zero-mean Gaussian noise term with unknown standard deviation  $\sigma_r$ , which  
 517 is a free parameter of the model.

518 Action selection (i.e. motor output  $u_t$ ) is done via the weighted mean of  $x_{j,t}$ :

$$u_t = \sum_j p(\zeta_{j,t}|q_t...)x_{j,t} \quad (6)$$

519 where  $p(\zeta_{j,t}|q_t...)$  is the predictive probability.

520 To include motor noise (independent from estimation uncertainty), as well as carry over  
 521 the uncertainty over  $x_{j,t}$ , we instead sample motor commands from a Gaussian centered on  
 522 this mean, with a standard deviation  $\sigma_u$ , which is a free parameter of the model.

523 **Simplified COIN model.** The free parameters of this model can be fitted to par-  
 524 ticipants' data, as was done by Heald et al. (2021). In this work, we instead chose values  
 525 for these parameters to show that the model is capable of explaining the experimental phe-  
 526 nomena in the Results section. Additionally, by fixing these parameters the agent is able to  
 527 perform exact Bayesian inference at each trial using conjugate priors, replacing the MCMC  
 528 approach used by Heald et al. (2021) due to the mathematical intractability of the full  
 529 formulation. This, however, does not significantly change the model and was done purely  
 530 for computational efficiency. In this section, we describe how we fixed parameters and the  
 531 procedure for Bayesian inference.

As explained above, context is assumed to be a discrete variable which evolves as a Markov process. The transition matrices  $\pi$  were generated via a Dirichlet process, with parameters that can be inferred from participant data ( $\alpha$  and  $\kappa$  in Heald et al. (2021)). For a fixed value of these parameters, the transition matrices also become fixed. In our simulations, we set the probability of self-transitioning (denoted  $p_\zeta$ ) depending on the experiments (see below), to numbers that approximate the experimental setup of each study.

Contextual cues are assumed by the agent to be sampled from a distribution that depends on the current context. This is done through a set of cue probability vectors that are generated via a parametric distribution, whose parameters are fitted to participants' data. For experiments that do not include probabilistic or deceiving cues, contextual cues, when present, unequivocally reflect the current context, i.e.  $p(q_t = i|c_t = j) = d_{ij}$ , where  $d_{ij}$  is the Kronecker delta, equaling one when  $i = j$ , zero otherwise. For the simulations of Figure 1, where contextual cues are probabilistic, cue uncertainty is implemented as  $p(c_t = i|q_t = i) = 1 - \eta$ , where  $\eta$  is the cue uncertainty, and  $p(c_t = i|q_t = j) = \eta/(N_c - 1) \forall i \neq j$ , where  $N_c$  is the total number of contexts in the experiment.

Using the above, the probability of a context for the state feedback for a trial after the cue has been observed is given by:

$$p(c_t|q_t, y_{1:t-1}) \propto p(c_t|q_t)p(c_t|c_{t-1})p(c_{t-1}|y_{1:t-1}) \quad (7)$$

where  $p(c_t|c_{t-1})$  is given by the context self-transition ( $p_\zeta$  in Table 1 below) such that:

$$p(c_t = i|c_{t-1} = j) = \begin{cases} p_\zeta & \text{if } i = j \\ \frac{1-p_\zeta}{N_c-1} & \text{otherwise} \end{cases} \quad (8)$$

Finally, for the hidden variables  $x_{j,t}$  we chose a stationary Gaussian distribution with unknown mean  $\mu_x$  and standard deviation  $\sigma_x$ , instead of the AR(1)  $a$  and  $d$  parameters used by Heald et al. (2021). As a consequence, the sCOIN model does not have intrinsic memory decay, instead relying on the dynamics of context inference to explain the slow decay of memories during error-clamp trials (e.g. Brennan & Smith, 2015; Scheidt et al., 2000; Vaswani & Shadmehr, 2013).

Using Bayesian inference, the model infers the values of  $\mu_x$  and  $\sigma_x$  using a Gaussian likelihood and NormalGamma priors, which allowed us to use exact inference. The likelihood of the data is given by the prediction error of the observations (which drives learning):

$$p(y_t|x_t) = \mathcal{N}(y - \hat{y}, \hat{\sigma}) \quad (9)$$

where  $\hat{y}$  is the predicted observation given the previous observation and the previous action, and  $\hat{\sigma}$  is the expected standard deviation of the predicted observation, given by the updated parameters of the model (discussed below).

We set priors over  $\mu_{\zeta,x}$  and  $\sigma_{\zeta,x}$  that enable exact inference over the latent variables  $x$  (in what follows, we dropped the  $j$  dependency for clarity):

$$\mu_x, \sigma_x \sim \mathcal{NG}(\mu_0, \nu_0, \alpha_0, \beta_0) \quad (10)$$

564 with free parameters  $\mu_0$ ,  $\nu_0$ ,  $\alpha_0$  and  $\beta_0$ , which we fixed for each experiment separately.  
 565 Because  $x$  is context-specific, so are these parameters. This formulation comes with four  
 566 free parameters (i.e. the hyper-priors  $\mu_{0,i}, \nu_{0,i}, \alpha_{0,i}, \beta_{0,i}$ ), in accordance with the original  
 567 formulation (note that Heald et al. (2021) fixed the mean of the priors for  $b$  to zero). While  
 568 the two formulations are not mathematically identical, the effects of the hyper-priors for  
 569 both are the same; we discuss these effects in the next section.

Because the likelihood function  $p(y_t|x_t, \dots)$  is Gaussian, this choice of priors allows us to calculate the update equations as follows:

$$\begin{aligned}\mu_{\phi,i}^{(t)} &= \frac{\nu_{\phi,i}^{(t-1)} \mu_{\phi,i}^{(t-1)} + p(\zeta_i|q_t, \dots) s_t}{\nu_{\phi,t}^{(t-1)} + p(\zeta_i|q_t, \dots)} \\ \nu_{\phi,t}^{(t)} &= \nu_{\phi,t}^{(t-1)} + p(\zeta_i|q_t, \dots) \\ \alpha_{\phi,t}^{(t)} &= \alpha_{\phi,i}^{(t-1)} + p(\zeta_i|q_t, \dots)/2 \\ \beta_{\phi,i}^{(t)} &= \beta_{\phi,i}^{(t-1)} + \frac{p(\zeta_i|q_t, \dots) \nu_{\phi,i}^{(t-1)}}{\nu_{\phi,i}^{(t-1)} + p(\zeta_i|q_t, \dots)} \frac{(s_t - \mu_{\phi,t}^{(t-1)})^2}{2}\end{aligned}\quad (11)$$

570 where  $s_t$  represents the observations, in the form of the error between the observed and expected outcomes of the motor command. Note that the effect of the evidence (i.e. observations)  
 571 on the inference over the context-dependent hidden states is gated by the probability  
 572 of each context  $p(\zeta_i|q_t, \dots)$ , as in (Heald et al., 2021, supplementary materials).

574 **Model parameters.** Table 1 lists all the parameter values that we used during our  
 575 simulations. The parameters are divided into two categories: (1) task parameters, which  
 576 encode the way we simulated the experimental design; (2) agent parameters, which cor-  
 577 respond to the free parameters listed in the previous section. The variable names for the  
 578 model parameters are given in the “Var” column, corresponding to the variables in the  
 579 previous section. The values are divided into experiments and, within experiments, into the  
 different groups or conditions that we simulated.

| Var         | Description     | Kim (2015)              | Oh (2019)        |           | Davidson (2004) |          | Vaswani (2013) |            |        |
|-------------|-----------------|-------------------------|------------------|-----------|-----------------|----------|----------------|------------|--------|
|             |                 |                         | Exp. 1           | Exp. 2    | Grp. 3A         | Grp. -A  | Grp. 1         | Grp. 2     | Grp. 3 |
| Task pars.  | Contextual cues | Yes                     |                  |           |                 | No       |                |            |        |
|             | $x_j^*$         | Adaptation sizes        | 0, 40, -40       | 0, 20     | 0, 10           | 0, 4, -4 | 0, 4, 12       | 1          | 0, 1   |
|             | $\sigma_a$      | Adaptation noise        | 0.01             |           | 1               |          | 0.5            |            | 0.1    |
|             | $\sigma_r^*$    | Obs. noise              | 3                |           | 2.5             |          | 0.1            |            | 0.1    |
| Agent pars. | $p_\zeta$       | Context self-transition | 0.9              | 0.98      |                 | 0.98     |                | 0.9        | 0.8    |
|             | $\mu_0$         |                         | 0, -1, 1         | 0, 0      | 0, 4, -4        | 0, 4, 12 | 0, 1           | 0, 1, -0.5 |        |
|             | $\nu_0$         | Hyper priors            | 1e4, 1, 1        | 1e4, 1    | 1e4, 1, 1       |          | 1e4, 1         | 1e4, 1, 1  |        |
|             | $\alpha_0$      |                         | 25e3, 0.25, 0.25 | 22e3, 2.2 | 33e3, 4e2, 4e2  |          | 5e4, 5         | 15e4, 5, 5 |        |
|             | $\beta_0$       |                         | 1e5, 2, 2        | 1e5, 20   | 1e5, 23e2, 23e2 |          | 1e5, 2         | 1e5, 2, 2  |        |
|             | $\sigma_u$      | Motor noise             | 1                |           | 2               |          |                | 0.17       |        |
|             | $\sigma_r$      | Obs. noise              | 3                | 2.5       |                 | 2.5      |                | 0.1        |        |

Table 1

*Model and simulation parameters.* The star notation (e.g.  $x_j^*$ ) denotes the real value used in the simulation of the task, which may be different from that assumed by the agent.

581 We estimated the task parameters from the information provided in their respective  
 582 publications; when direct information was not provided, we estimated it from the reported  
 583 results; these estimations are not exact, but function as a proof of concept. Agent parameter  
 584 values are held constant for the different conditions or groups for each experiment, except  
 585 those parameters that are expected to vary across conditions.

586 Because the sCOIN model does not have a mechanism for the online creation of new  
 587 contexts, relying instead of a fixed number of contexts, the number of existing contexts  
 588 was set according to each experiment. For the experiments by Kim et al. (2015), to aid  
 589 in learning of the two adaptations, the  $\mu_0$  hyperparameters were set to -1 and 1 (plus the  
 590 baseline of zero), which lead to the model learning the -40 and 40 visuomotor rotation angles,  
 591 respectively. As the experiments by Oh and Schweighofer (2019) have only one adaptation,  
 592 this was not necessary and the new context was initiated with  $\mu_0 = 0$ . For the rest of  
 593 the simulated experiments the focus was not on learning, but on the switching between  
 594 known contexts, therefore we started simulations with models that had already learned the  
 595 adaptations, setting the learned values to the real values used in each experiment.

596 The hyperparameters  $\alpha_0$  and  $\beta_0$  were set first for the baseline context such that the  
 597 expected standard deviation of observations  $\beta/\alpha$  roughly matched the observation noise in  
 598 the task, i.e.  $\beta_0/\alpha_0 \sim \sigma_r + \sigma_u$ , while keeping the values for  $\beta_0$  and  $\alpha_0$  very high, which,  
 599 together with the high  $\nu_0$  values, ensure that learning in this context is very slow. For the  
 600 other contexts, the ratio  $\beta_0/\alpha_0$  was set to be higher than the baseline, while keeping the  
 601 individual values  $\alpha_0$  and  $\beta_0$  much lower, to speed up learning.

602 The exact values for  $\alpha_0$  and  $\beta_0$  were set for each experiment such that  $\beta_0/\alpha_0 = 2*(\sigma_r\sigma_a)$ ,  
 603 where  $\sigma_a$  is the standard deviation of the adaptation. The rationale behind this choice is  
 604 that  $\sigma_r$  and  $\sigma_a$  determine the noise in the observations made by the model at each trial, and  
 605 their sum is the value of  $\beta/\alpha$  to which the learning process converges with enough trials.  
 606 We multiplied it by 2 in order to help in learning, specifically to make the *a priori* standard  
 607 deviation higher for the untrained contexts than for the baseline context.

608 Of important note is the difference between the true observation noise and the expected  
 609 observation noise in the simulations for the Davidson and Wolpert (2004) experiments. The  
 610 expected observation noise  $\sigma_r$  was set to a higher value to reflect the fact that feedback  
 611 in curl-force mechanical arm experiments, while devoid of any added noise, is more diffi-  
 612 cult for people to use to inform adaptation than in other types of experiments due to the  
 613 nonlinear nature of the force. This fact is reflected in the high number of trials necessary  
 614 for full adaptation in these experiments as compared to, for example, visuomotor rotation  
 615 experiments.

616 For the simulations in Figure 1, the parameters were set as in the experiments by  
 617 Davidson and Wolpert (2004), with two exceptions: (1) the cue uncertainty, which is set  
 618 to the values of 0 and 0.33, for the low and high values, respectively; and (2) the agent’s  
 619 observation noise  $\sigma_r$ , with values of 0.5 and 2.

620     **Interpreting the hyper-parameters.**  $\mu$  determines the initial estimate of the adaptation  
 621     in the same units as the necessary adaptation.  $\nu$  encodes how stable this hyper-prior  
 622     is: higher values (e.g. 10,000) all but guarantee that the hyper-prior  $\mu$  will not change its  
 623     value after observations; In principle, enough evidence should still modify it, but that would  
 624     not happen during an experiment. Smaller values (i.e.  $\sim 1$ ) make  $\mu$  follow evidence more  
 625     freely. Note that as more observations are accumulated,  $\nu$  becomes bigger and bigger,  
 626     stabilizing the value of  $\mu$ .

627     The hyper-parameters  $\alpha$  and  $\beta$  have a more complex effect. Note that the mean of a  
 628     gamma distribution is  $\beta/\alpha$ ; this mean is being used as the standard deviation of a Gaussian  
 629     by the rest of the agent, which makes it an important measure of uncertainty. While setting  
 630     the default hyper-parameters, the values used are, e.g.,  $\alpha = 0.5/\sigma_0$  and  $\beta = 0.5$ , where  $\sigma_0$   
 631     is the *a priori* estimate of the standard deviation of the force exerted by the environment,  
 632     which controls the initial learning rate. This makes the initial standard deviation equal  $\sigma_0$ ,  
 633     which makes it consistent with the fixed-force model. The 0.5 values ensure that uncertainty  
 634     is large at the beginning and is greatly reduced during the experiment, but never to a point  
 635     where it is so small that it makes trial-to-trial variation in the environment surprising.  
 636     Changing this 0.5 would make the standard deviation change more quickly, making the  
 637     model more or less precise in its predictions, independently of the volatility of the mean of  
 638     the adaptation (via  $\mu$ ).

639     The baseline model defaults to different values that make it a lot more stable. The  
 640     hyper-standard deviation of the mean is set to 10,000, which makes the mean entirely  
 641     stable during the duration of the experiment. The values of  $\alpha$  and  $\beta$  are fixed regardless of  
 642      $\sigma_0$  such that the standard deviation is 0.001 (compared that to the size of the adaptations  
 643     in mechanical arm experiments, around 0.0125), and the hyper-parameters of the standard  
 644     deviation are stable during the experiment.

645

## Acknowledgment

646     Funded by the German Research Foundation (DFG, Deutsche Forschungsgemeinschaft)  
 647     as part of Germany’s Excellence Strategy – EXC 2050/1 – Project ID 390696704 – Cluster  
 648     of Excellence “Centre for Tactile Internet with Human-in-the-Loop” (CeTI) of Technische  
 649     Universität Dresden.

650

## References

- 651     Behrens, T. E. J., Woolrich, M. W., Walton, M. E., & Rushworth, M. F. S. (2007, September).  
 652         Learning the value of information in an uncertain world. *Nature Neuroscience*, 10(9), 1214–  
 653         1221. doi: 10.1038/nrn1954
- 654     Brashers-Krug, T., Shadmehr, R., & Bizzi, E. (1996, July). Consolidation in human motor memory.  
 655         *Nature*, 382(6588), 252–255. doi: 10.1038/382252a0
- 656     Brennan, A. E., & Smith, M. A. (2015, June). The Decay of Motor Memories Is Independent of  
 657         Context Change Detection. *PLoS Computational Biology*, 11(6), e1004278. doi: 10.1371/jour-  
 658         nal.pcbi.1004278

- 659 Criscimagna-Hemminger, S. E., & Shadmehr, R. (2008, September). Consolidation Patterns  
660 of Human Motor Memory. *Journal of Neuroscience*, 28(39), 9610–9618. doi:  
661 10.1523/JNEUROSCI.3071-08.2008
- 662 Davidson, P. R., & Wolpert, D. M. (2004, November). Scaling down motor memories:  
663 De-adaptation after motor learning. *Neuroscience Letters*, 370(2-3), 102–107. doi:  
664 10.1016/j.neulet.2004.08.003
- 665 Dizio, P., & Lackner, J. R. (1995, October). Motor adaptation to Coriolis force perturbations of  
666 reaching movements: Endpoint but not trajectory adaptation transfers to the nonexposed  
667 arm. *Journal of Neurophysiology*, 74(4), 1787–1792. doi: 10.1152/jn.1995.74.4.1787
- 668 Ernst, M. O., & Banks, M. S. (2002, January). Humans integrate visual and haptic information in  
669 a statistically optimal fashion. *Nature*, 415(6870), 429–433. doi: 10.1038/415429a
- 670 Ethier, V., Zee, D. S., & Shadmehr, R. (2008, May). Spontaneous Recovery of Motor Mem-  
671 ory During Saccade Adaptation. *Journal of Neurophysiology*, 99(5), 2577–2583. doi:  
672 10.1152/jn.00015.2008
- 673 Forano, M., & Franklin, D. W. (2020, October). Timescales of motor memory formation in  
674 dual-adaptation. *PLOS Computational Biology*, 16(10), e1008373. doi: 10.1371/jour-  
675 nal.pcbi.1008373
- 676 Gandolfo, F., Mussa-Ivaldi, F. A., & Bizzi, E. (1996, April). Motor learning by field ap-  
677 proximation. *Proceedings of the National Academy of Sciences*, 93(9), 3843–3846. doi:  
678 10.1073/pnas.93.9.3843
- 679 Heald, J. B., Lengyel, M., & Wolpert, D. M. (2021, December). Contextual inference underlies the  
680 learning of sensorimotor repertoires. *Nature*, 600(7889), 489–493. doi: 10.1038/s41586-021-  
681 04129-3
- 682 Herzfeld, D. J., Kojima, Y., Soetedjo, R., & Shadmehr, R. (2018, May). Encoding of error and  
683 learning to correct that error by the Purkinje cells of the cerebellum. *Nature Neuroscience*,  
684 21(5), 736–743. doi: 10.1038/s41593-018-0136-y
- 685 Herzfeld, D. J., Vaswani, P. A., Marko, M. K., & Shadmehr, R. (2014, September). A memory of  
686 errors in sensorimotor learning. *Science*, 345(6202), 1349–1353. doi: 10.1126/science.1253138
- 687 Howard, I. S., Ingram, J. N., Franklin, D. W., & Wolpert, D. M. (2012, September). Gone in 0.6  
688 Seconds: The Encoding of Motor Memories Depends on Recent Sensorimotor States. *Journal*  
689 *of Neuroscience*, 32(37), 12756–12768. doi: 10.1523/JNEUROSCI.5909-11.2012
- 690 Howard, I. S., Ingram, J. N., & Wolpert, D. M. (2010, October). Context-Dependent Partitioning  
691 of Motor Learning in Bimanual Movements. *Journal of Neurophysiology*, 104(4), 2082–2091.  
692 doi: 10.1152/jn.00299.2010
- 693 Huang, V. S., & Shadmehr, R. (2009, August). Persistence of Motor Memories Reflects  
694 Statistics of the Learning Event. *Journal of Neurophysiology*, 102(2), 931–940. doi:  
695 10.1152/jn.00237.2009
- 696 Imamizu, H., Sugimoto, N., Osu, R., Tsutsui, K., Sugiyama, K., Wada, Y., & Kawato, M. (2007,  
697 August). Explicit contextual information selectively contributes to predictive switching of  
698 internal models. *Experimental Brain Research*, 181(3), 395–408. doi: 10.1007/s00221-007-  
699 0940-1
- 700 Kim, S., Ogawa, K., Lv, J., Schweighofer, N., & Imamizu, H. (2015, December). Neural Substrates  
701 Related to Motor Memory with Multiple Timescales in Sensorimotor Adaptation. *PLOS*  
702 *Biology*, 13(12), e1002312. doi: 10.1371/journal.pbio.1002312
- 703 Kording, K. P., & Wolpert, D. M. (2004, January). Bayesian integration in sensorimotor learning.  
704 *Nature*, 427(6971), 244–247. doi: 10.1038/nature02169
- 705 Lee, J.-Y., & Schweighofer, N. (2009, August). Dual Adaptation Supports a Parallel Ar-  
706 chitecture of Motor Memory. *Journal of Neuroscience*, 29(33), 10396–10404. doi:  
707 10.1523/JNEUROSCI.1294-09.2009
- 708 Marko, M. K., Haith, A. M., Harran, M. D., & Shadmehr, R. (2012, September). Sensitivity to  
709 prediction error in reach adaptation. *Journal of Neurophysiology*, 108(6), 1752–1763. doi:

- 710 10.1152/jn.00177.2012
- 711 Medina, J. F., Garcia, K. S., & Mauk, M. D. (2001, June). A Mechanism for Savings in the  
712 Cerebellum. *Journal of Neuroscience*, 21(11), 4081–4089. doi: 10.1523/JNEUROSCI.21-11-  
713 04081.2001
- 714 Nassar, M. R., McGuire, J. T., Ritz, H., & Kable, J. W. (2019, February). Dissociable Forms of  
715 Uncertainty-Driven Representational Change Across the Human Brain. *Journal of Neuro-  
716 science*, 39(9), 1688–1698. doi: 10.1523/JNEUROSCI.1713-18.2018
- 717 Oh, Y., & Schweighofer, N. (2019, November). Minimizing Precision-Weighted Sensory Prediction  
718 Errors via Memory Formation and Switching in Motor Adaptation. *Journal of Neuroscience*,  
719 39(46), 9237–9250. doi: 10.1523/JNEUROSCI.3250-18.2019
- 720 Pekny, S. E., Criscimagna-Hemminger, S. E., & Shadmehr, R. (2011, September). Protection and  
721 Expression of Human Motor Memories. *The Journal of Neuroscience*, 31(39), 13829–13839.  
722 doi: 10.1523/JNEUROSCI.1704-11.2011
- 723 Scheidt, R. A., Dingwell, J. B., & Mussa-Ivaldi, F. A. (2001, August). Learning to Move Amid  
724 Uncertainty. *Journal of Neurophysiology*, 86(2), 971–985. doi: 10.1152/jn.2001.86.2.971
- 725 Scheidt, R. A., Reinkensmeyer, D. J., Conditt, M. A., Rymer, W. Z., & Mussa-Ivaldi, F. A. (2000,  
726 August). Persistence of motor adaptation during constrained, multi-joint, arm movements.  
727 *Journal of Neurophysiology*, 84(2), 853–862. doi: 10.1152/jn.2000.84.2.853
- 728 Scholz, J. P., & Schöner, G. (1999, May). The uncontrolled manifold concept: Identifying con-  
729 trol variables for a functional task. *Experimental Brain Research*, 126(3), 289–306. doi:  
730 10.1007/s002210050738
- 731 Shadmehr, R., & Brashers-Krug, T. (1997, January). Functional Stages in the Formation  
732 of Human Long-Term Motor Memory. *Journal of Neuroscience*, 17(1), 409–419. doi:  
733 10.1523/JNEUROSCI.17-01-00409.1997
- 734 Shadmehr, R., & Mussa-Ivaldi, F. A. (1994, May). Adaptive representation of dynamics during  
735 learning of a motor task. *The Journal of Neuroscience: The Official Journal of the Society  
736 for Neuroscience*, 14(5 Pt 2), 3208–3224.
- 737 Shmuelof, L., Huang, V. S., Haith, A. M., Delnicki, R. J., Mazzoni, P., & Krakauer, J. W. (2012, Oc-  
738 tober). Overcoming Motor “Forgetting” Through Reinforcement Of Learned Actions. *Journal  
739 of Neuroscience*, 32(42), 14617–14621a. doi: 10.1523/JNEUROSCI.2184-12.2012
- 740 Smith, M. A., Ghazizadeh, A., & Shadmehr, R. (2006, June). Interacting Adaptive Processes  
741 with Different Timescales Underlie Short-Term Motor Learning. *PLoS Biology*, 4(6). doi:  
742 10.1371/journal.pbio.0040179
- 743 Vaswani, P. A., & Shadmehr, R. (2013, May). Decay of Motor Memories in the Absence of Error.  
744 *Journal of Neuroscience*, 33(18), 7700–7709. doi: 10.1523/JNEUROSCI.0124-13.2013
- 745 Zarahn, E., Weston, G. D., Liang, J., Mazzoni, P., & Krakauer, J. W. (2008, November). Explain-  
746 ing Savings for Visuomotor Adaptation: Linear Time-Invariant State-Space Models Are Not  
747 Sufficient. *Journal of Neurophysiology*, 100(5), 2537–2548. doi: 10.1152/jn.90529.2008